THE ASTROPHYSICAL JOURNAL, 392:470–484, 1992 June 20

STEPS TOWARD DETERMINATION OF THE SIZE AND STRUCTURE OF THE BROAD-LINE REGION IN ACTIVE GALACTIC NUCLEI. III. FURTHER OBSERVATIONS OF NGC 5548 AT OPTICAL WAVELENGTHS[1]

B. M. PETERSON,[2] D. ALLOIN,[3] D. AXON,[4] T. J. BALONEK,[5] R. BERTRAM,[2,6] T. A. BOROSON,[7]
J. A. CHRISTENSEN,[5,8] S. D. CLEMENTS,[9] M. DIETRICH,[10] M. ELVIS,[11] A. V. FILIPPENKO,[12]
C. M. GASKELL,[13,14] C. A. HASWELL,[15] J. P. HUCHRA,[11] N. JACKSON,[4]
W. KOLLATSCHNY,[10] K. T. KORISTA,[2,16] N. J. LAME,[2] R. J. LEACOCK,[9]
S.-N. LIN,[17] M. A. MALKAN,[18] A. S. MONK,[19] M. V. PENSTON,[19,20]
R. W. POGGE,[2] A. ROBINSON,[21] E. I. ROSENBLATT,[22]
J. C. SHIELDS,[12,23] A. G. SMITH,[9] G. M. STIRPE,[24]
W.-H. SUN,[17] T. J. TURNER,[25] R. M. WAGNER,[2,6]
B. J. WILKES,[11] AND B. J. WILLS[15]

Received 1991 October 8; accepted 1991 December 27

ABSTRACT

We report on the results of the second year of an intensive ground-based spectroscopic and photometric study of variability in the bright Seyfert 1 galaxy NGC 5548, which has been undertaken in order to study the relationship between continuum and emission-line variability. Relative to the first year of the monitoring program, the nucleus of NGC 5548 was considerably fainter and the continuum variations slower during the second year, but the continuum-Hβ cross-correlation results for the two years are nearly identical. The variations in the broad Hβ emission line lag behind those in the continuum by somewhat less than 20 days, as concluded from the first year's data.

Subject headings: galaxies: individual (NGC 5548) — galaxies: Seyfert — quasars: emission lines

1. INTRODUCTION

Continuum and emission-line variability in active galactic nuclei (AGNs) provides a valuable tool for probing the inner structure of these spatially unresolved sources. In practice, extracting information about the nature of the AGN continuum source and the emission-line regions from variability observations is difficult because of the large amount of high-quality data required. Given the apparently nonperiodic nature of the continuum variability and rapid response of the emission lines to continuum changes, the continuum and emission-line light curves must be sampled frequently over an extended period of time. This constitutes a demanding observational program, particularly since moderate-resolution spectroscopy of faint AGNs must be carried out with reasonably large telescopes. Recognition of the practical difficulties of such a program on the one hand and of the potential scientific return on the other has led us to a large-scale cooperative effort to monitor intensively the spectrum of NGC 5548, a bright Seyfert 1 galaxy. Our initial results, based on a several-month program of ultraviolet (Clavel et al. 1991, hereafter Paper I) and optical (Peterson et al. 1991, hereafter Paper II) monitoring of continuum and emission-line flux variations in this galaxy, showed that the broad emission lines undergo the same variations as the continuum, but with a short time delay,

[1] This paper is dedicated to the memory of our colleague, coauthor, and friend, Dr. Michael V. Penston, who passed away on 1990 December 23. Michael was pioneer in AGN variability studies and in extragalactic observations with *IUE*. He played a key role in the organization of several AGN monitoring consortia, including this one. He will be missed by all of us.

[2] Department of Astronomy, Ohio State University, 174 West 18th Avenue, Columbus, OH 43210.
[3] Observatoire de Paris, URA173 CNRS, 92195 Meudon, France.
[4] University of Manchester, Nuffield Radio Astronomy Laboratories, Macclesfield, Cheshire, England SK11 9DL, UK.
[5] Department of Physics and Astronomy, Colgate University, Hamilton, NY 13346.
[6] Mailing address: Lowell Observatory, Mars Hill Road, 1400 West, Flagstaff, AZ 86001.
[7] Kitt Peak National Observatory, National Optical Astronomy Observatories, P.O. Box 26732, Tucson, AZ 85726.
[8] Mailing address: Space Telescope Science Institute, 3700 San Martin Drive, Baltimore, MD 21218.
[9] Department of Astronomy, University of Florida, Gainesville, FL 32611.
[10] Universitäts-Sternwarte Göttingen, Geismarlandstrasse 11, D-3400 Göttingen, Germany.
[11] Harvard-Smithsonian Center for Astrophysics, 60 Garden Street, Cambridge, MA 02138.
[12] Department of Astronomy, University of California, Berkeley, CA 94720.
[13] Department of Astronomy, University of Michigan, Ann Arbor, MI 48109.
[14] Mailing address: Department of Physics and Astronomy, University of Oklahoma, Norman, OK 73019.
[15] McDonald Observatory and Department of Astronomy, University of Texas, RLM 15.308, Austin, TX 78712.
[16] Mailing address: Observatories of the Carnegie Institution of Washington, 813 Santa Barbara Street, Pasadena, CA 91101.
[17] Institute of Physics and Astronomy, National Central University, 32054 Chung-Li, Taiwan.
[18] Department of Astronomy, University of California, Math-Science Building, Los Angeles, CA 90024.
[19] Royal Greenwich Observatory, Madingley Road, Cambridge, England, CB3 0EZ, UK.
[20] Deceased, 1990 December 23.
[21] Institute of Astronomy, Madingley Road, Cambridge, England, CB3 0HA, UK.
[22] Center for Astrophysics and Space Sciences, University of California at San Diego, C-011, La Jolla, CA 92093.
[23] Mailing address: Department of Astronomy, Ohio State University, 174 West 18th Avenue, Columbus, OH 43210.
[24] Osservatorio Astronomico di Bologna, Via Zamboni 33, I-40126, Bologna, Italy.
[25] Laboratory for High Energy Astrophysics, NASA Goddard Space Flight Center, Code 668, Greenbelt, MD 20771.

or lag, which is attributed to light-travel time effects in the broad-line region (BLR). Indeed, each emission line responds with a different lag, with the highest ionization lines responding most rapidly to the continuum variations. This has been taken to be evidence for ionization stratification within the BLR.

There are a number of reasons that it is highly desirable to extend this intensive monitoring program beyond the original campaign, which ran from 1988 December to 1989 October (hereafter referred to as "Year 1"). There is historical evidence that a wider range of continuum variability takes place over longer intervals of time, i.e., the variability power spectrum extends to lower frequencies than sampled in the original campaign. Also, there are pronounced emission-line profile variations, the nature of which is not clearly understood, that are observed on longer time scales. It is hoped that some insight into the origin of line profile variation might be obtained by spectroscopic monitoring over the BLR dynamical time scale, $t_{\rm dyn} = R/\Delta v_{\rm FWHM} \approx 3$ yr, where R is the size of the BLR from variability studies ($\sim$20 light days, Paper II), and $\Delta v_{\rm FWHM}$ is the width of the emission-line profile ($\sim$5000 km s^{-1}). Indeed, changes in the BLR response time itself might be possible on time scales of a few years, depending on the geometry and velocity field of the line-emitting gas.

In this contribution, we report on an extension of the ground-based monitoring campaign on NGC 5548 during the period 1989 December through 1990 October (hereafter referred to as "Year 2"). We present the optical spectroscopy and photometry in § 2. In § 3, we outline the procedures by which we construct a homogeneous data base from these observations to produce light curves for the optical continuum and the Hβ emission line. Simple time-series analysis is performed in § 4, and we compare the results obtained here with the results of Paper II. Our major conclusions are summarized in § 5. Also included in this paper are revised continuum measurements for the year 1 spectra (Appendix A) and several additional spectra from Year 1 (Appendix B).

2. OBSERVATIONS

2.1. *Optical Spectroscopy*

A complete log of spectroscopic observations appears in Table 1. The UT date and Julian date of each observation are given in columns (1) and (2), respectively. The column (3) entry gives a code which indicates the observatory and instrument used to obtain the spectrum. These codes are unchanged from Paper II wherever possible. The projected spectrograph entrance aperture, in arcseconds, is given in column (4). The first dimension is the slit width in the dispersion direction, and the second dimension is the slit length in the cross-dispersion direction; in the case of CCDs, the second entry is the "extraction window" used. The slit position angle is given in column (5), measured eastward from north; the cross-dispersion direction runs north–south for a position angle 0°. An estimate of the seeing, when it was recorded at the telescope, is given in column (6). The nominal spectral resolution is given in column (7), and column (8) contains the approximate wavelength range covered by the data. Finally, to aid future investigators who will make use of these data, column (9) gives a unique identifier by which the spectrum is known to the IRAF reduction system, and which is contained in the FITS file header. The file naming convention is the same as used in the Year 1 study: the first two characters ("n5") identify the galaxy as NGC 5548, and the next four characters (e.g., "7861") contain the four least significant figures in the Julian date, as in column (2). The next character gives the observatory code, as in column (3). When necessary, an additional arbitrary character is added to eliminate any remaining ambiguity.

2.2. *Photometry*

A program of photographic photometry was carried out with the 0.76 m telescope of the Rosemary Hill Observatory of the University of Florida in Bronson, Florida. Photographs were obtained in three colors: U (Kodak 103a-O + UG-2), B (Kodak 103a-O + GG-385), and V (Kodak 103a-D + GG-495). The data were recorded and measured as described in Paper II. The results are given in Table 2.

Broad-band photometric measurements were also obtained with a Photometrics liquid-nitrogen cooled CCD system with a Thomson 7882 chip on the 0.4 m telescope of Foggy Bottom Observatory of Colgate University. The combination of the CCD response and the blue (Mould) filter (kindly loaned by Kitt Peak National Observatory) approximates Johnson B. During the later part of the campaign, this filter was replaced with a custom filter designed by D. Beckert which has a somewhat narrower band response than the Mould filter, similar to that described by Beckert & Newberry (1989). The integrated magnitudes inside a circular aperture of diameter 17.″5, centered on the nucleus of the galaxy, are given in Table 3. Star 1 from Penston, Penston, & Sandage (1971) was used as a comparison star. A more detailed description of the filter system and presentation of data in other bandpasses will be given elsewhere.

3. ANALYSIS OF THE DATA

As in Paper II, we will at this time confine our attention only to those spectra in Table 1 which cover the Hβ spectral region. Further analysis will be left to future papers.

3.1. *Absolute Calibration of the Spectra*

Absolute flux calibration of the optical spectra has been accomplished by taking the flux in the narrow emission lines to be constant over the time scales of interest, as was done in Paper II and as is common in AGN variability studies. In the Hβ region of the spectrum, [O III] λ5007 is especially useful for flux calibration purposes as it is strong and usually not strongly contaminated by other spectral features; in general, the strongest contaminant is Fe II λ5018, which does not appear to be strong in NGC 5548. Furthermore, its proximity to Hβ mitigates the effects of any wavelength-dependent calibration errors. In Paper II, we obtained the absolute flux in the [O III] λ5007 line by averaging measurements made through large spectrograph entrance apertures on nights which were reported to be photometric by the observers. In order to verify the [O III] λ5007 absolute flux reported in Paper II and to check our assumption that the [O III] λ5007 flux does not vary on short time scales, we have repeated this analysis for the Year 2 data. The [O III] λ5007 flux, transformed to the rest frame of NGC 5548 ($z = 0.0174$), is given in Table 4 for those spectra from Table 1 which were obtained through large apertures on photometric nights. These data are in excellent agreement with the Year 1 results. We continue to use the absolute flux given in Paper II in order to keep all of the measurements for both years on the same flux scale.

TABLE 1

LOG OF SPECTROSCOPIC OBSERVATIONS

UT Date (1)	Julian Date (2,440,000+) (2)	Code (3)	Aperture Size (4)	Aperture P.A. (5)	Seeing (6)	Resolution (Å) (7)	Range (Å) (8)	IRAF File (9)
1989 Dec 1	7861	H	4.0 × 10.0	119	1.5	10	3420–6310	n57861h
1989 Dec 8	7868	A	5.0 × 7.6	90	3	9	4590–5730	n57686a
1989 Dec 24	7884	A	5.0 × 7.6	90	2	9	4500–5640	n57884a
1989 Dec 31	7891	A	5.0 × 7.6	90	5	9	4500–5640	n57891a
1990 Jan 3	7895	H	4.0 × 10.0	130	3–4	10	3430–7560	n57895h
1990 Jan 4	7896	F	3.2 × 6.4	90		5	4550–7050	n57896f
1990 Jan 5	7897	F	3.2 × 6.4	90		5	4550–7050	n57897f
1990 Jan 8	7899	A	5.0 × 7.6	90	5	9	4580–5700	n57899a
1990 Jan 9	7900	A	5.0 × 7.6	90	5	9	4560–5700	n57900a
1990 Jan 10	7901	A	5.0 × 7.6	90	3–4	9	4560–5700	n57901a
1990 Jan 16	7907	R	1.7 × 5.0	0	1.5	5	4470–5540	n57907r
1990 Jan 17	7908	R	1.7 × 5.0	0	1.5	5	6060–7140	n57908r
1990 Jan 19	7910	N	8.8 × 6.8	0	2–2.5	13	4320–6940	n57910n
1990 Jan 20	7912	F	3.2 × 6.4	90		5	4550–7050	n57912f
1990 Jan 20	7912	H	4.0 × 10.0	160	1.5	10	3430–6280	n57912h
1990 Jan 20	7912	N	8.8 × 12.2	0	2–2.5	13	4350–6070	n57912na
1990 Jan 20	7912	N	8.8 × 10.8	0	2–2.5	13	5710–7040	n57912nb
1990 Jan 24	7915	A	5.0 × 7.6	90	3–4	9	4560–5690	n57915a
1990 Jan 26	7918	F	3.2 × 6.4	90		5	4550–7050	n57918f
1990 Jan 27	7919	F	3.2 × 6.4	90		5	4550–7050	n57919f
1990 Jan 29	7921	F	3.2 × 6.4	90		5	4550–7050	n57921f
1990 Jan 30	7922	F	3.2 × 6.4	90		5	4550–7050	n57922f
1990 Feb 4	7927	F	3.2 × 6.4	90		5	4550–7050	n57927f
1990 Feb 7	7929	A	5.0 × 7.6	90	3–4	9	4530–5710	n57929a
1990 Feb 17	7940	F	3.2 × 6.4	90		5	4550–7050	n57940f
1990 Feb 18	7941	F	3.2 × 6.4	90		5	4550–7050	n57941f
1990 Feb 22	7945	F	3.2 × 6.4	90		5	4550–7050	n57945f
1990 Feb 23	7945	O	1.9 × 4.7	65	2	3.5	6210–7220	n57945o
1990 Feb 23	7946	F	3.2 × 6.4	90		5	4550–7050	n57946fa
1990 Feb 24	7946	F	3.2 × 6.4	90		5	4520–7050	n57946fb
1990 Feb 25	7947	F	3.2 × 6.4	90		5	4520–7050	n5794f
1990 Feb 27	7949	A	5.0 × 7.6	90	2–3	9	4570–5720	n57949a
1990 Feb 28	7951	F	3.2 × 6.4	90		5	4520–7050	n57951f
1990 Mar 5	7955	F	3.2 × 64	90		5	4580–7050	n57955f
1990 Mar 7	7957	A	5.0 × 7.6	90	5	9	4580–5720	n57957a
1990 Mar 8	7958	A	5.0 × 7.6	90	4–5	9	4610–5750	n57958a
1990 Mar 17	7967	F	3.2 × 6.4	90		5	4550–7050	n57967f
1990 Mar 18	7968	F	3.2 × 6.4	90		5	4580–7050	n57968f
1990 Mar 19	7969	F	3.2 × 6.4	90		5	4550–7050	n57969f
1990 Mar 20	7970	F	3.2 × 6.4	90		5	4550–7050	n57970f
1990 Mar 21	7971	A	5.0 × 7.6	90	2–3	9	4620–5640	n57971a
1990 Mar 21	7971	F	3.2 × 6.4	90		5	4550–7050	n57971f
1990 Mar 23	7973	F	3.2 × 6.4	90		5	4550–7050	n57973f
1990 Mar 24	7974	F	3.2 × 6.4	90		5	4580–7050	n57974f
1990 Mar 25	7975	F	3.2 × 6.4	90		5	4550–7050	n57975f
1990 Mar 25	7975	H	4.0 × 10.0	60	2–3	20	3960–7080	n57975h
1990 Mar 30	7980	F	3.2 × 6.4	90		5	4580–7050	n57980f
1990 Apr 1	7982	A	5.0 × 7.6	90	4	9	4530–5670	n57982a
1990 Apr 1	7982	F	3.2 × 6.4	90		5	4580–7050	n57982f
1990 Apr 1	7982	H	4.0 × 10.0	59	1–1.5	20	3960–7080	n57982h
1990 Apr 3	7984	T	1.9 × 10.0	160		5	4600–5500	n57984ta
1990 Apr 3	7984	T	1.9 × 10.0	160		3	6240–7080	n57984tb
1990 Apr 9	7990	A	5.0 × 7.6	90	3–4	9	4520–5660	n57990a
1990 Apr 13	7994	A	5.0 × 7.6	90	3	9	4540–5670	n57994aa
1990 Apr 13	7994	A	5.0 × 7.6	90	3	9	6010–7160	n57994ab
1990 Apr 13	7994	A	5.0 × 7.6	90	3	9	5290–6440	n57994ac
1990 Apr 16	7997	C	1.5 × 10.0	0	3	7	6280–7200	n57997c
1990 Apr 18	7999	F	3.2 × 6.4	90		5	4580–7050	n57999f
1990 Apr 21	8002	F	3.2 × 6.4	90		5	4580–7050	n58002f
1990 Apr 23	8004	U	1.8 × 6.0	90	2	8	3500–7580	n58004u
1990 Apr 24	8005	F	3.2 × 6.4	90		5	4550–7050	n58005f
1990 Apr 24	8005	O	1.6 × 7.8	90	2	5	3450–5450	n58005o
1990 Apr 26	8007	A	5.0 × 7.6	90	2–3	9	4540–5680	n58007a
1990 Apr 26	8007	F	3.2 × 6.4	90		5	4550–7050	n58007f
1990 Apr 27	8008	F	3.2 × 6.4	90		5	4580–7050	n58008f
1990 Apr 28	8009	F	3.2 × 6.4	90		5	4580–7050	n58009f
1990 Apr 30	8011	H	4.0 × 10.0	61	3	10	3420–7570	n58011h
1990 May 2	8013	A	5.0 × 7.6	90	3–4	9	4580–5680	n58013a

TABLE 1—*Continued*

UT Date (1)	Julian Date (2,440,000+) (2)	Code (3)	Aperture Size (4)	Aperture P.A. (5)	Seeing (6)	Resolution (Å) (7)	Range (Å) (8)	IRAF File (9)
1990 May 9	8020	A	5.0 × 7.6	90	4	9	4520–5620	n58020aa
1990 May 9	8020	A	5.0 × 7.6	90	4	9	5920–7070	n58020ab
1990 May 17	8028	A	5.0 × 7.6	90	2–3	9	4530–5660	n58028aa
1990 May 17	8028	A	5.0 × 7.6	90	2–3	9	6010–7010	n58028ab
1990 May 19	8030	F	3.2 × 6.4	90		5	4580–7050	n58030f
1990 May 20	8031	F	3.2 × 6.4	90		5	4580–7050	n58031f
1990 May 21	8032	F	3.2 × 6.4	90		5	4550–7050	n58032f
1990 May 23	8034	F	3.2 × 6.4	90		5	4580–7050	n58034f
1990 May 25	8036	F	3.2 × 6.4	90		5	4580–7050	n58036f
1990 May 26	8037	A	5.0 × 7.6	90	3–4	9	4540–5670	n58037a
1990 May 26	8037	F	3.2 × 6.4	90		5	4550–7050	n58037f
1990 May 28	8039	F	3.2 × 6.4	90		5	4550–7050	n58039f
1990 May 29	8040	F	3.2 × 6.4	90		5	4550–7050	n58040f
1990 May 30	8041	F	3.2 × 6.4	90		5	4580–7050	n58041f
1990 May 31	8042	F	3.2 × 6.4	90		5	4550–7050	n58024f
1990 Jun 1	8043	F	3.2 × 6.4	90		5	4580–7050	n58043f
1990 Jun 2	8044	A	5.0 × 7.6	90	3–4	9	4290–5430	n58044a
1990 Jun 5	8047	C	1.5 × 10.0	160		6	4580–5500	n58047ca
1990 Jun 5	8047	C	1.5 × 10.0	160		7	6280–7200	n58047cb
1990 Jun 8	8050	C	1.5 × 10.0	160		7	6290–7200	n58050c
1990 Jun 9	8051	S	5.0 × 4.0	90	1–2	10	4400–6800	n58051s
1990 Jun 14	8056	H	4.0 × 10.0	61	2	10	3130–9880	n58056h
1990 Jun 17	8059	F	3.2 × 6.4	90		5	4580–7050	n58059f
1990 Jun 18	8060	F	3.2 × 6.4	90		5	4580–7050	n58060f
1990 Jun 19	8061	A	5.0 × 7.6	90	2	9	4290–5430	n58061aa
1990 Jun 19	8061	A	5.0 × 7.6	90	2	9	5990–7140	n58061ab
1990 Jun 19	8061	F	3.2 × 6.4	90		5	4580–7050	n58061f
1990 Jun 19	8061	N	8.8 × 13.6	0	2–2.5	13	4400–7020	n58061n
1990 Jun 20	8062	N	8.8 × 12.8	90	2–2.5	13	4400–7020	n58062n
1990 Jun 22	8064	F	3.2 × 6.4	90		5	4580–7050	n58064f
1990 Jun 25	8067	F	3.2 × 6.4	90		5	4580–7050	n58067f
1990 Jun 26	8068	A	5.0 × 7.6	90	2–3	9	4510–5640	n58068a
1990 Jun 26	8068	F	3.2 × 6.4	90		5	4550–7050	n58068f
1990 Jul 5	8077	A	5.0 × 7.6	90	2	9	4430–5570	n58077a
1990 Jul 16	8089	M	2.0 × 10.0	90	2–3	7	4000–7250	n58089m
1990 Jul 17	8089	H	4.0 × 10.0	58	2	10	3130–7510	n58089h
1990 Jul 18	8090	A	5.0 × 7.6	90	2–3	9	4470–5610	n58090a
1990 Jul 19	8091	F	3.2 × 6.4	90		5	4610–7050	n58091f
1990 Jul 20	8092	N	8.8 × 12.6	0	2–2.5	13	4330–6870	n58092n
1990 Jul 25	8097	A	5.0 × 7.6	90	2–3	9	4530–5670	n58097a
1990 Jul 25	8097	F	3.2 × 6.4	90		5	4580–7050	n58097f
1990 Jul 30	8102	H	4.0 × 10.0	61	1	10	3110–7520	n58102h
1990 Aug 17	8120	K	3.1 × 3.0	0	2	12	4830–7740	n58120k
1990 Aug 25	8128	A	5.0 × 7.6	90	2–3	9	4420–5650	n58128a
1990 Aug 29	8132	H	4.0 × 10.0	58	1.5	10	3150–6110	n58132h
1990 Aug 30	8133	H	4.0 × 10.0	58	2	20	3920–9900	n58133h
1990 Sep 9	8143	A	5.0 × 7.6	90	2–3	9	4530–5660	n58143a
1990 Sep 14	8148	A	5.0 × 7.6	90	2–3	9	4540–5680	n58148a
1990 Sep 17	8151	A	5.0 × 7.6	90	2–3	9	4530–5670	n58151a
1990 Sep 26	8160	A	5.0 × 7.6	90	2–3	9	4540–5680	n58160a
1990 Oct 6	8170	K	8.7 × 3.0	0	1.5–2	16	4790–7600	n58170ka
1990 Oct 6	8170	K	2.2 × 3.0	0	1.5–2	12	4790–7600	n58170kb
1990 Oct 7	8171	K	2.2 × 3.0	0	1.5–2	12	4790–7600	n58171k
1990 Oct 15	8179	A	5.0 × 7.6	90	2–3	9	4510–5640	n58179a

NOTE.—Codes for Data Origin. A: 1.8 m Perkins Telescope + Ohio State CCD spectrograph.
C: 2.5 m Isaac Newton Telescope + CCD.
F: 1.6 m Mount Hopkins Telescope + Reticon scanner.
H: 3.0 m Shane Telescope + UV Schmidt spectrograph.
J: 2.7 m McDonald Telescope + Cassegrain grating spectrograph.
K: 2.4 m MDM Telescope + Mark IIIb CCD spectrograph.
M: 3.5 m and 2.2 m Calar Alto Observatory + CCD spectrographs.
N: 1.0 m Nickel Telescope, Lick Observatory + CCD spectrograph.
O: 2.1 m Telescope, Kitt Peak National Observatory + Gold Camera.
R: 1.5 m Loiano Telescope + CCD.
S: 1.5 m CTIO Telescope + CCD.
T: 4.2 m William Herschel Telescope + CCD.
U: 1.9 m SAAO Telescope + Reticon.

TABLE 2

PHOTOGRAPHIC PHOTOMETRY

UT Date (1)	Julian Date (2,440,000+) (2)	U (3)	B (4)	V (5)
1990 Jan 27	7918	13.89 ± 0.09	14.51 ± 0.10	13.93 ± 0.24
1990 Feb 28	7950	14.02 ± 0.14	14.41 ± 0.14	14.06 ± 0.29
1990 Mar 24	7974	14.33 ± 0.05	14.79 ± 0.09	...
1990 Apr 5	7986	...	14.77 ± 0.06	...
1990 Apr 16	7997	13.92 ± 0.15	14.49 ± 0.07	14.03 ± 0.12
1990 Apr 26	8007	13.82 ± 0.15	14.41 ± 0.14	...
1990 May 26	8037	13.83 ± 0.16	14.46 ± 0.14	14.33 ± 0.16
1990 May 27	8038	...	14.27 ± 0.10	...
1990 May 29	8040	14.11 ± 0.28	14.12 ± 0.11	14.15 ± 0.21
1990 May 30	8041	13.57 ± 0.14	14.33 ± 0.12	14.31 ± 0.10
1990 Jun 13	8055	...	14.17 ± 0.10	13.89 ± 0.15
1990 Jun 14	8056	13.56 ± 0.10	14.18 ± 0.10	14.14 ± 0.16
1990 Jun 20	8062	...	14.44 ± 0.13	14.19 ± 0.18

3.2. *Spectral Measurements*

Continuum and Hβ emission-line measurements were made from the spectra listed in Table 1 as described in Paper II, but with one important change. In order to reduce the contribution of various emission features to the reported continuum measurements, we have chosen to measure the continuum flux at 5100 Å, a local minimum between the Hβ + [O III] complex and the Fe II λ5250 blend, rather than at 4870 Å, as in Paper II. In order to provide continuum measurements for both years on a common scale, all of the spectra presented in Paper II have been remeasured, and the 5100 Å continuum values for Year 1 are given in Appendix A.

Each set of data, as designated by the individual codes in column (3) of Table 1, was treated as being homogeneous. The flux ratios F_λ(5100 Å)/F([O III] λ5007) and F(Hβ)/F([O III] λ5007) were measured for each of the spectra in Table 1 in which these features appear. The emission-line fluxes were measured as described in Paper II. The flux ratios are given in Table 5, grouped by individual homogeneous data set. The continuum and Hβ fluxes can be placed on an absolute scale by multiplying each ratio by the adopted [O III] λ5007 flux, i.e., $F_{5007} = 5.58 \times 10^{-13}$ ergs s^{-1} cm^{-2}.

TABLE 3

CCD PHOTOMETRY

UT Date (1)	Julian Date (2,440,000+) (2)	Filter Code[a] (3)	B (4)
1990 Feb 1	7923	1	14.34 ± 0.01
1990 Feb 21	7943	1	14.36 ± 0.01
1990 Mar 7	7957	1	14.40 ± 0.02
1990 Mar 28	7978	1	14.43 ± 0.01
1990 Apr 13	7994	1	14.26 ± 0.03
1990 Apr 14	7995	1	14.30 ± 0.01
1990 Apr 17	7998	1	14.31 ± 0.02
1990 Apr 19	8000	1	14.30 ± 0.01
1990 Apr 23	8004	1	14.30 ± 0.01
1990 Apr 23	8004	2	14.29 ± 0.02
1990 Apr 24	8005	1	14.27 ± 0.02
1990 May 12	8023	2	14.24 ± 0.02
1990 May 25	8036	2	14.22 ± 0.02
1990 May 27	8038	2	14.16 ± 0.02
1990 May 28	8039	2	14.15 ± 0.03
1990 May 31	8042	2	14.11 ± 0.03
1990 Jun 1	8043	2	14.18 ± 0.02
1990 Jun 2	8044	2	14.18 ± 0.04
1990 Jun 8	8050	2	14.16 ± 0.03
1990 Jun 22	8064	2	14.26 ± 0.03
1990 Jun 26	8068	2	14.29 ± 0.03
1990 Jun 27	8069	2	14.39 ± 0.04
1990 Jun 28	8070	2	14.36 ± 0.06
1990 Jul 3	8075	2	14.31 ± 0.02
1990 Jul 7	8079	2	14.39 ± 0.02
1990 Jul 17	8089	2	14.29 ± 0.04
1990 Jul 25	8097	2	14.32 ± 0.03
1990 Jul 26	8098	2	14.29 ± 0.03
1990 Jul 30	8102	2	14.32 ± 0.04
1990 Aug 15	8118	2	14.22 ± 0.03
1990 Aug 16	8119	2	14.16 ± 0.04
1990 Sep 9	8143	2	14.31 ± 0.03
1990 Oct 28	8192	2	14.31 ± 0.02

[a] Filter Codes: 1 = Mould, 2 = Beckert.

3.3. *Intercalibration of the Data*

Each of the individual sets of measurements given in Table 5 is internally quite homogeneous, and the larger data sets show the same qualitative pattern of variability. However, there are small differences or offsets between the different data sets

TABLE 4

ABSOLUTE CALIBRATION CHECK

F([O III] λ5007) (10^{-13} ergs cm^{-2} s^{-1}) (1)	Aperture Size (2)	File name (3)
5.75	8.8 × 6.8	n57910n
5.56	8.8 × 12.2	n57912na
5.53	4.0 × 10.0	n57975h
5.61	4.0 × 10.0	n57982h
5.43	5.0 × 7.6	n58037a
5.53	4.0 × 10.0	n58056h
5.15	5.0 × 7.6	n58061aa
5.31	8.8 × 13.6	n58061n
5.89	8.8 × 12.8	n58062n
5.25	5.0 × 7.6	n58090a
5.70	8.8 × 12.6	n58092n
5.69	4.0 × 10.0	n58102h
5.11	5.0 × 7.6	n58151a
5.26	5.0 × 7.6	n58160a
5.48 ± 0.24	Mean value from Year 2	
5.58 ± 0.27	Mean value from Year 1	(adopted absolute flux)

TABLE 5

MEASUREMENTS OF SPECTRA

Julian Date (2,440,000+) (1)	$100F_\lambda$(5100 Å) / F([O III] λ5007) (2)	F(Hβ) / F([O III] λ5007) (3)	IRAF File (4)
A. Ohio State CCD			
7868.....	1.84	1.57	n57868a
7884.....	1.58	1.63	n57884a
7891.....	1.45	1.45	n57891a
7899.....	1.52	1.44	n57899a
7900.....	1.47	1.47	n57900a
7901.....	1.44	1.46	n57901a
7915.....	1.29	1.30	n57915a
7929.....	1.08	1.05	n57929a
7949.....	1.11	1.05	n57949a
7957.....	1.11	0.87	n57957a
7958.....	1.04	0.92	n57958a
7971.....	0.98	0.79	n57971a
7982.....	1.06	0.73	n77982a
7990.....	1.16	0.71	n57990a
7994.....	1.23	0.80	n57994aa
8007.....	1.30	0.90	n58007a
8013.....	1.44	0.90	n58013a
8020.....	1.42	1.04	n58020aa
8028.....	1.45	1.09	n58028aa
8037.....	1.42	1.10	n58037a
8044.....	1.48	1.21	n58044a
8061.....	1.38	1.25	n58061aa
8068.....	1.25	1.16	n58068a
8077.....	1.17	1.02	n58077a
8090.....	1.21	0.91	n58090a
8097.....	1.27	0.92	n58097a
8128.....	1.36	1.22	n58128a
8143.....	1.29	1.11	n58143a
8148.....	1.35	1.06	n58148a
8151.....	1.32	1.02	n58151a
8160.....	1.41	1.04	n58160a
8179.....	1.70	1.17	n58179a
C—INT CCD			
8047.....	1.17	1.14	n58047ca
F–SAO Reticon			
7896.....	1.22	1.68	n57896f
7897.....	1.23	1.68	n57897f
7912.....	1.07	1.41	n57912f
7918.....	0.97	1.54	n57918f
7919.....	1.00	1.37	n57919f
7921.....	0.98	1.23	n57921f
7922.....	0.95	1.27	n57922f
7927.....	0.90	1.11	n57927f
7940.....	0.99	1.04	n57940f
7941.....	0.90	1.08	n57941f
7945.....	1.00	1.04	n57945f
7946.....	0.94	1.03	n57946fa
7946.....	1.04	1.05	n57946fb
7947.....	0.93	1.10	n57947f
7951.....	0.95	1.01	n57951f
7955.....	1.00	0.91	n57955f
7967.....	0.82	0.87	n57967f
7968.....	0.86	0.97	n57968f
7969.....	0.84	0.87	n57969f
7970.....	0.97	0.88	n57970f
7971.....	0.87	0.84	n57971f
7973.....	0.83	0.88	n57973f
7974.....	0.83	0.87	n57974f
7975.....	0.91	0.80	n57975f
7980.....	1.00	0.87	n57980f
7982.....	0.88	0.80	n57982f
7999.....	1.06	1.02	n57999f
8002.....	1.06	0.99	n58002f
8005.....	1.17	1.07	n58005f
8007.....	1.04	1.03	n58007f
8008.....	1.08	1.15	n58008f
F–SAO Reticon			
8009.....	1.20	1.07	n58009f
8030.....	1.21	1.26	n58030f
8031.....	1.22	1.25	n58031f
8032.....	1.20	1.33	n58032f
8034.....	1.16	1.35	n58034f
8036.....	1.22	1.27	n58036f
8037.....	1.34	1.40	n58037f
8039.....	1.23	1.30	n58039f
8040.....	1.31	1.14	n58040f
8041.....	1.29	1.20	n58041f
8042.....	1.26	1.34	n58042f
8043.....	1.16	1.34	n58043f
8059.....	1.14	1.31	n58059f
8060.....	1.18	1.41	n58060f
8061.....	1.10	1.17	n58061f
8064.....	1.16	1.32	n58064f
8067.....	1.02	1.32	n58067f
8068.....	1.06	1.26	n58068f
8091.....	1.07	1.01	n58091f
8097.....	1.00	1.08	n58097f
H—Lick Shane CCD			
7861.....	1.80	1.43	n57861h
7895.....	1.40	1.54	n57895h
7912.....	1.12	1.30	n57912h
7975.....	1.02	0.84	n57975h
7982.....	1.05	0.78	n57982h
8011.....	1.43	0.96	n58011h
8056.....	1.40	1.22	n58056h
8089.....	1.17	0.96	n58089h
8102.....	1.24	0.94	n58102h
8132.....	1.22	1.20	n58132h
8133.....	1.27	1.12	n58133h
K—Michigan CCD			
8120.....	1.45	1.15	n58120k
8170.....	1.66	1.07	n58170ka
8170.....	1.62	1.11	n58170kb
8171.....	1.55	0.95	n58171k
M—Calar Alto CCD			
8089.....	1.10	0.93	n58089m
N—Lick Nickel CCD			
7910.....	1.71	1.29	n57910n
7912.....	1.95	1.36	n57912na
8061.....	2.00	1.27	n58061n
8062.....	1.93	1.23	n58062n
8092.....	1.38	0.92	n58092n
O—KPNO CCD			
8005.....	0.98	1.03	n58005o
R—Loiano CCD			
7907.....	1.05	1.49	n57907r
S—CTIO CCD			
8051.....	1.76	1.25	n58051s
T—Wm. Herschel CCD			
7984.....	0.88	0.77	n57984ta
U—SAAO Reticon			
8004.....	1.13	0.96	n58004u

which we attribute to aperture effects. Aperture effects occur because of the differences in the surface brightness distributions of the various physical components (the nonstellar continuum, the BLR, the narrow-line region, and the underlying stellar background) which contribute to the nuclear spectra of AGNs; different aperture geometries admit different relative amounts of each of these. Within individual data sets, seeing effects (as well as centering and guiding errors) are important because the amount of light from each of the physical components entering the spectrograph varies with the point-spread function. This is almost certainly the largest source of uncertainty in the flux measurements.

Following the procedure detailed in Paper II, we make an empirical correction for these aperture effects by comparing data from different sets which are nearly contemporaneous, and by assuming that the differences between the data sets are due entirely to aperture effects. We define a point-source correction factor φ by the equation

$$F(\mathrm{H}\beta) = \varphi F_{5007}\left[\frac{F(\mathrm{H}\beta)}{F([\mathrm{O\ III}]\ \lambda 5007)}\right]_{\mathrm{obs}}, \quad (1)$$

where F_{5007} is the absolute [O III] λ5007 flux, and the observed ratio is as given in Table 5. We also define an extended source correction G to the continuum flux which accounts for the differences in the amount of starlight admitted through different apertures,

$$F_\lambda(5100\ \text{Å}) = \varphi F_{5007}\left[\frac{F_\lambda(5100\ \text{Å})}{F([\mathrm{O\ III}]\ \lambda 5007)}\right]_{\mathrm{obs}} - G\,. \quad (2)$$

The intercalibration process consists of comparing pairs of nearly simultaneous observations from different data sets to determine for each data set the values of the constants φ and G which are needed to adjust the emission-line and continuum fluxes to a common scale. Furthermore, the formal uncertainties in φ and G reflect the uncertainties in the individual data sets, so we can determine the nominal uncertainties for each data set if we assume that the errors add in quadrature.

In Paper II, the constants φ and G were determined by comparing pairs of points from different data sets which are separated by no more than two days, as we have found no evidence for variability on time scales this short. The intercalibration procedure is carried out by first comparing some of the larger data sets, and then gradually building up the intercalibrated data base by including additional data sets. All the data are calibrated relative to data set A because these data are fairly numerous, overlap reasonably well with most of the other data sets, and were obtained through a reasonably large aperture (5″ × 7″.6).

Fractional uncertainties in the continuum [$\sigma_{\mathrm{cont}}/F_\lambda(5100\ \text{Å}) \approx 0.040$] and the H$\beta$ flux [$\sigma_{\mathrm{line}}/F(\mathrm{H}\beta) \approx 0.035$] are adopted for the similar, large-aperture, high-quality data sets A and H, as in Paper II, since the Year 2 data from these sources are of the same quality as the Year 1 data. However, the internal errors of the set F data have been reassessed for Year 2 as in general these data have lower signal-to-noise ratios in Year 2, which is attributable to the fact that NGC 5548 was typically ~25% fainter during Year 2 than in Year 1. The fractional uncertainties in set F, estimated as in Paper II by comparing pairs of measurements separated by 2 days or less, are found to be $\sigma_{\mathrm{cont}}/F_\lambda(5100\ \text{Å}) \approx 0.055$ and $\sigma_{\mathrm{line}}/F(\mathrm{H}\beta) \approx 0.055$.

For most of the other data sets, it was possible to estimate the mean uncertainties in the measurements by comparing them to measurements from other sets for which the uncertainties are known and by assuming that the uncertainties for each set add in quadrature. This procedure did not work well for some of the small data sets, and in such cases we simply adopted uncertainties from the larger data sets which were most similar in terms of spectrograph entrance aperture, spectral resolution, and signal-to-noise ratio. The short time scale sampling in the Year 2 data is not quite as good as in the Year 1 data described in Paper II, and it was therefore necessary to relax some of our assumptions in a few cases: For sets C and M it was necessary to consider pairs of points separated by up to 4 days to obtain reliable intercalibration constants, and for sets R and S intervals of 5 days were allowed. The most important difficulty encountered is that none of the observations in set K were obtained close enough in time to any of the other observations to use our usual intercalibration method. For set K, we therefore used the intercalibration constants for this set from Paper II[26].

TABLE 6

FLUX SCALE FACTORS

Data Set (1)	Point Source Scale Factor φ (2)	Extended Source Correction G (10^{-15} ergs s^{-1} cm^{-2} Å^{-1}) (3)
A.....	1.000	0.000
C.....	1.058 ± 0.005	−0.937 ± 0.585
F.....	0.897 ± 0.064	−1.625 ± 0.438
H.....	0.949 ± 0.039	−0.540 ± 0.298
K.....	0.983 ± 0.048	−1.106 ± 1.237
M.....	0.969 ± 0.017	−0.856 ± 0.119
N.....	0.953 ± 0.059	2.989 ± 0.449
O.....	0.901 ± 0.029	−2.262 ± 0.331
R.....	0.843 ± 0.021	−1.796 ± 0.561
S.....	0.946 ± 0.027	1.387 ± 0.077
T.....	0.947 ± 0.015	−1.365 ± 0.093
U.....	0.964 ± 0.037	−1.124 ± 0.275

The intercalibration constants we use for each data set are given in Table 6, and these constants are used with equations (1) and (2) to adjust the measurements given in Table 5 to a common flux scale, which corresponds to measurements through the 5″ × 7″.6 spectrograph entrance aperture used in set A. The resultant values of the continuum flux F_λ(5100 Å) and the line flux $F(\mathrm{H}\beta)$ are given in Table 7, and a final light curve is produced by computing the variance-weighted average of all the measurements obtained on a given Julian date, as given in Table 8.

In Figure 1, we show the continuum light curve as given in Table 8, as well as the B-band photometric measurements from Tables 2 and 3, which have been placed on an approximate flux scale by using the relationship

$$B = -2.5 \log (F_\nu) - 48.60 \quad (3)$$

(Oke & Gunn 1983), where F_ν is the flux in units of ergs s^{-1} cm^{-2} Hz^{-1}. Inspection of the F_λ(5100 Å) light curve in the third panel of Figure 1 suggests that the continuum point at JD 2,448,120 might be too high; this is a reasonable concern because this measurement is from set K, for which the intercalibration is less certain, as described above. However, the fact that the B-band CCD photometry in the middle

[26] The constant G has been reevaluated for all of the Year 1 data because of the redefined continuum wavelength. These values are given in Appendix A.

TABLE 7

SCALED FLUX MEASUREMENTS

Julian Date (2,440,000+) (1)	Code (2)	F_λ(5100 Å) (10^{-15} ergs s^{-1} cm^{-2} Å^{-1}) (3)	F(Hβ) (10^{-13} ergs s^{-1} cm^{-2}) (4)	Julian Date (2,440,000+) (1)	Code (2)	F_λ(5100 Å) (10^{-15} ergs s^{-1} cm^{-2} Å^{-1}) (3)	F(Hβ) (10^{-13} ergs s^{-1} cm^{-2}) (4)
7861.....	H	10.07 ± 0.40	7.57 ± 0.26	8007.....	A	7.25 ± 0.29	5.02 ± 0.18
7868.....	A	10.27 ± 0.41	8.76 ± 0.31	8007.....	F	6.83 ± 0.38	5.16 ± 0.28
7884.....	A	8.82 ± 0.35	9.10 ± 0.32	8008.....	F	7.03 ± 0.39	5.76 ± 0.32
7891.....	A	8.09 ± 0.32	8.09 ± 0.28	8009.....	F	7.63 ± 0.42	5.36 ± 0.29
7895.....	H	7.95 ± 0.32	8.15 ± 0.28	8011.....	H	8.11 ± 0.32	5.08 ± 0.18
7896.....	F	7.73 ± 0.43	8.41 ± 0.46	8013.....	A	8.03 ± 0.32	5.02 ± 0.18
7897.....	F	7.78 ± 0.43	8.41 ± 0.46	8020.....	A	7.92 ± 0.32	5.80 ± 0.20
7899.....	A	8.48 ± 0.34	8.03 ± 0.28	8028.....	A	8.09 ± 0.32	6.08 ± 0.21
7900.....	A	8.20 ± 0.33	8.20 ± 0.29	8030.....	F	7.68 ± 0.42	6.31 ± 0.35
7901.....	A	8.03 ± 0.32	8.15 ± 0.28	8031.....	F	7.73 ± 0.43	6.26 ± 0.34
7907.....	R	6.74 ± 0.50	7.01 ± 0.28	8032.....	F	7.63 ± 0.42	6.66 ± 0.37
7910.....	N	6.11 ± 0.24	6.86 ± 0.27	8034.....	F	7.43 ± 0.41	6.76 ± 0.37
7912.....	F	6.98 ± 0.38	7.06 ± 0.39	8036.....	F	7.73 ± 0.43	6.36 ± 0.35
7912.....	N	7.38 ± 0.29	7.23 ± 0.29	8037.....	F	8.33 ± 0.46	7.01 ± 0.38
7912.....	H	6.47 ± 0.26	6.88 ± 0.24	8037.....	A	7.92 ± 0.32	6.14 ± 0.22
7915.....	A	7.20 ± 0.29	7.25 ± 0.25	8039.....	F	7.78 ± 0.43	6.51 ± 0.36
7918.....	F	6.48 ± 0.36	7.71 ± 0.42	8040.....	F	8.18 ± 0.45	5.71 ± 0.31
7919.....	F	6.63 ± 0.37	6.86 ± 0.38	8041.....	F	8.08 ± 0.44	6.01 ± 0.33
7921.....	F	6.53 ± 0.36	6.16 ± 0.34	8042.....	F	7.93 ± 0.44	6.71 ± 0.37
7922.....	F	6.38 ± 0.35	6.36 ± 0.35	8043.....	F	7.43 ± 0.41	6.71 ± 0.37
7927.....	F	6.13 ± 0.34	5.56 ± 0.31	8044.....	A	8.26 ± 0.33	6.75 ± 0.24
7929.....	A	6.03 ± 0.24	5.86 ± 0.20	8047.....	C	7.84 ± 0.47	6.73 ± 0.30
7940.....	F	6.58 ± 0.36	5.20 ± 0.29	8051.....	S	7.90 ± 0.32	6.60 ± 0.26
7941.....	F	6.13 ± 0.34	5.41 ± 0.30	8056.....	H	7.95 ± 0.32	6.46 ± 0.23
7945.....	F	6.63 ± 0.37	5.20 ± 0.29	8059.....	F	7.33 ± 0.40	6.56 ± 0.36
7946.....	F	6.33 ± 0.35	5.16 ± 0.28	8060.....	F	7.53 ± 0.41	7.06 ± 0.39
7946.....	F	6.83 ± 0.38	5.26 ± 0.29	8061.....	A	7.70 ± 0.31	6.97 ± 0.24
7947.....	F	6.28 ± 0.34	5.51 ± 0.30	8061.....	N	7.65 ± 0.31	6.75 ± 0.27
7949.....	A	6.19 ± 0.25	5.86 ± 0.20	8061.....	F	7.13 ± 0.39	5.86 ± 0.32
7951.....	F	6.38 ± 0.35	5.05 ± 0.28	8062.....	N	7.27 ± 0.29	6.54 ± 0.26
7955.....	F	6.63 ± 0.37	4.55 ± 0.25	8064.....	F	7.43 ± 0.41	6.61 ± 0.36
7957.....	A	6.19 ± 0.25	4.86 ± 0.17	8067.....	F	6.73 ± 0.37	6.61 ± 0.36
7958.....	A	5.80 ± 0.23	5.13 ± 0.18	8068.....	F	6.93 ± 0.38	6.31 ± 0.35
7967.....	F	5.73 ± 0.31	4.36 ± 0.24	8068.....	A	6.97 ± 0.28	6.47 ± 0.23
7968.....	F	5.93 ± 0.33	4.86 ± 0.27	8077.....	A	6.53 ± 0.25	5.69 ± 0.20
7969.....	F	5.83 ± 0.32	4.36 ± 0.24	8089.....	H	6.74 ± 0.27	5.08 ± 0.18
7970.....	F	6.48 ± 0.36	4.40 ± 0.24	8089.....	M	6.80 ± 0.51	5.03 ± 0.20
7971.....	A	5.47 ± 0.22	4.41 ± 0.15	8090.....	A	6.75 ± 0.27	5.08 ± 0.18
7971.....	F	5.98 ± 0.33	4.20 ± 0.23	8091.....	F	6.98 ± 0.38	5.05 ± 0.28
7973.....	F	5.78 ± 0.32	4.40 ± 0.24	8092.....	N	6.74 ± 0.27	4.89 ± 0.20
7974.....	F	5.78 ± 0.32	4.36 ± 0.24	8097.....	A	7.09 ± 0.28	5.13 ± 0.18
7975.....	H	5.94 ± 0.24	4.45 ± 0.16	8097.....	F	6.63 ± 0.37	5.41 ± 0.30
7975.....	F	6.18 ± 0.34	4.00 ± 0.22	8102.....	H	7.11 ± 0.28	4.98 ± 0.17
7980.....	F	6.63 ± 0.37	4.36 ± 0.24	8120.....	K	9.06 ± 0.68	6.31 ± 0.22
7982.....	A	5.91 ± 0.24	4.07 ± 0.14	8128.....	A	7.59 ± 0.30	6.81 ± 0.24
7982.....	F	6.03 ± 0.33	4.00 ± 0.22	8132.....	H	7.00 ± 0.28	6.36 ± 0.22
7982.....	H	6.10 ± 0.24	4.13 ± 0.14	8133.....	H	7.27 ± 0.29	5.93 ± 0.21
7983.....	T	6.01 ± 0.45	4.07 ± 0.16	8143.....	A	7.20 ± 0.29	6.19 ± 0.22
7990.....	A	6.47 ± 0.26	3.96 ± 0.14	8148.....	A	7.53 ± 0.30	5.91 ± 0.21
7994.....	A	6.86 ± 0.28	4.46 ± 0.16	8151.....	A	7.37 ± 0.29	5.69 ± 0.20
7999.....	F	6.93 ± 0.38	5.11 ± 0.28	8160.....	A	7.87 ± 0.31	5.80 ± 0.20
8002.....	F	6.93 ± 0.38	4.95 ± 0.27	8170.....	K	10.21 ± 0.77	5.87 ± 0.20
8004.....	U	7.20 ± 0.29	5.16 ± 0.21	8170.....	K	9.99 ± 0.75	6.09 ± 0.21
8005.....	F	7.48 ± 0.41	5.36 ± 0.29	8171.....	K	9.61 ± 0.72	5.21 ± 0.18
8005.....	O	7.19 ± 0.43	5.18 ± 0.23	8179.....	A	9.49 ± 0.38	6.53 ± 0.23

panel of Figure 1 as well as V-band CCD photometry (to be published elsewhere) also shows high continuum values on JD 2,448,118–9 is reassuring.

As noted in Paper II, we can perform a final check of our uncertainty estimates by examining the ratios of all pairs of observations in Table 8 which are separated by 2 days or less. In Table 8, there are 72 independent pairs of measurements within 2 days of one another. The dispersion about the mean (unity), divided by $(2)^{1/2}$, provides an estimate of the typical uncertainty in a single measurement. For the continuum, we find that the mean fractional error in a given measurement is 0.035. The average fractional uncertainty, from the quoted estimates for these same 72 measurements in Table 8, is 0.046. This implies that our uncertainty estimates are probably quite good, and perhaps slightly overestimated. Examination of the Hβ emission-line fluxes indicates that the fractional uncertainty is 0.044, in very good agreement with the value of 0.042 computed from the Table 8 entries.

TABLE 8

OPTICAL CONTINUUM AND Hβ LIGHT CURVES

Julian Date (2,440,000+) (1)	F_λ(5100 Å) (10^{-15} ergs s^{-1} cm^{-2} Å^{-1}) (2)	F(Hβ) (10^{-13} ergs s^{-1} cm^{-2}) (3)	Julian Date (2,440,000+) (1)	F_λ(5100 Å) (10^{-15} ergs s^{-1} cm^{-2} Å^{-1}) (2)	F(Hβ) (10^{-13} ergs s^{-1} cm^{-2}) (3)
7861.....	10.07 ± 0.40	7.57 ± 0.26	8007.....	7.10 ± 0.23	5.06 ± 0.15
7868.....	10.27 ± 0.41	8.76 ± 0.31	8008.....	7.03 ± 0.39	5.76 ± 0.32
7884.....	8.82 ± 0.35	9.10 ± 0.32	8009.....	7.63 ± 0.42	5.36 ± 0.29
7891.....	8.09 ± 0.32	8.09 ± 0.28	8011.....	8.11 ± 0.32	5.08 ± 0.18
7895.....	7.95 ± 0.32	8.15 ± 0.28	8013.....	8.03 ± 0.32	5.02 ± 0.18
7896.....	7.73 ± 0.43	8.41 ± 0.46	8020.....	7.92 ± 0.32	5.80 ± 0.20
7897.....	7.78 ± 0.43	8.41 ± 0.46	8028.....	8.09 ± 0.32	6.08 ± 0.21
7899.....	8.48 ± 0.34	8.03 ± 0.28	8030.....	7.68 ± 0.42	6.31 ± 0.35
7900.....	8.20 ± 0.33	8.20 ± 0.29	8031.....	7.73 ± 0.43	6.26 ± 0.34
7901.....	8.03 ± 0.32	8.15 ± 0.28	8032.....	7.63 ± 0.42	6.66 ± 0.37
7907.....	6.74 ± 0.50	7.01 ± 0.28	8034.....	7.43 ± 0.41	6.76 ± 0.37
7910.....	6.11 ± 0.24	6.86 ± 0.27	8036.....	7.73 ± 0.43	6.36 ± 0.35
7912.....	6.89 ± 0.17	7.03 ± 0.17	8037.....	8.06 ± 0.26	6.34 ± 0.19
7915.....	7.20 ± 0.29	7.25 ± 0.25	8039.....	7.78 ± 0.43	6.51 ± 0.36
7918.....	6.48 ± 0.36	7.71 ± 0.42	8040.....	8.18 ± 0.45	5.71 ± 0.31
7919.....	6.63 ± 0.37	6.86 ± 0.38	8041.....	8.08 ± 0.44	6.01 ± 0.33
7921.....	6.53 ± 0.36	6.16 ± 0.34	8042.....	7.93 ± 0.44	6.71 ± 0.37
7922.....	6.38 ± 0.35	6.36 ± 0.35	8043.....	7.43 ± 0.41	6.71 ± 0.37
7927.....	6.13 ± 0.34	5.56 ± 0.31	8044.....	8.26 ± 0.33	6.75 ± 0.24
7929.....	6.03 ± 0.24	5.86 ± 0.20	8047.....	7.84 ± 0.47	6.73 ± 0.30
7940.....	6.58 ± 0.36	5.20 ± 0.29	8051.....	7.90 ± 0.32	6.60 ± 0.26
7941.....	6.13 ± 0.34	5.41 ± 0.30	8056.....	7.95 ± 0.32	6.46 ± 0.23
7945.....	6.63 ± 0.37	5.20 ± 0.29	8059.....	7.33 ± 0.40	6.56 ± 0.36
7946.....	6.56 ± 0.26	5.20 ± 0.20	8060.....	7.53 ± 0.41	7.06 ± 0.39
7947.....	6.28 ± 0.34	5.51 ± 0.30	8061.....	7.55 ± 0.19	6.63 ± 0.16
7949.....	6.19 ± 0.25	5.86 ± 0.20	8062.....	7.27 ± 0.29	6.54 ± 0.26
7951.....	6.38 ± 0.35	5.05 ± 0.28	8064.....	7.43 ± 0.41	6.61 ± 0.36
7955.....	6.63 ± 0.37	4.55 ± 0.25	8067.....	6.73 ± 0.37	6.61 ± 0.36
7957.....	6.19 ± 0.25	4.86 ± 0.17	8068.....	6.96 ± 0.23	6.42 ± 0.19
7958.....	5.80 ± 0.23	5.13 ± 0.18	8077.....	6.53 ± 0.26	5.69 ± 0.20
7967.....	5.73 ± 0.31	4.36 ± 0.24	8089.....	6.75 ± 0.24	5.06 ± 0.13
7968.....	5.93 ± 0.33	4.86 ± 0.27	8090.....	6.75 ± 0.27	5.08 ± 0.18
7969.....	5.83 ± 0.32	4.36 ± 0.24	8091.....	6.98 ± 0.38	5.05 ± 0.28
7970.....	6.48 ± 0.36	4.40 ± 0.24	8092.....	6.74 ± 0.27	4.89 ± 0.20
7971.....	5.63 ± 0.18	4.35 ± 0.13	8097.....	6.92 ± 0.22	5.21 ± 0.15
7973.....	5.78 ± 0.32	4.40 ± 0.24	8102.....	7.11 ± 0.28	4.98 ± 0.17
7974.....	5.78 ± 0.32	4.36 ± 0.24	8120.....	9.06 ± 0.68	6.31 ± 0.22
7975.....	6.02 ± 0.19	4.30 ± 0.13	8128...	7.59 ± 0.30	6.81 ± 0.24
7980.....	6.63 ± 0.37	4.36 ± 0.24	8132.....	7.00 ± 0.28	6.36 ± 0.22
7982.....	6.01 ± 0.15	4.08 ± 0.09	8133.....	7.27 ± 0.29	5.93 ± 0.21
7984.....	6.01 ± 0.45	4.07 ± 0.16	8143.....	7.20 ± 0.29	6.19 ± 0.22
7990.....	6.47 ± 0.26	3.96 ± 0.14	8148.....	7.53 ± 0.30	5.91 ± 0.21
7994.....	6.86 ± 0.28	4.46 ± 0.16	8151.....	7.37 ± 0.29	5.69 ± 0.20
7999.....	6.93 ± 0.38	5.11 ± 0.28	8160.....	7.87 ± 0.31	5.80 ± 0.20
8002.....	6.93 ± 0.38	4.95 ± 0.27	8170.....	10.10 ± 0.54	5.97 ± 0.15
8004.....	7.20 ± 0.29	5.16 ± 0.21	8171.....	9.61 ± 0.72	5.21 ± 0.18
8005.....	7.34 ± 0.30	5.25 ± 0.18	8179.....	9.49 ± 0.38	6.53 ± 0.23

4. VARIABILITY ANALYSIS

4.1. *Characteristics of the Data Base*

The 5100 Å continuum and Hβ emission-line light curves from Table 8 are shown in Figure 2. These data cover 94 separate epochs over a 319 day period. In Figure 3, the combined data from Year 1 (as given in Appendix A) and Year 2 are shown. The gap between the end of Year 1 and the beginning of Year 2 is 52 days, and the combined data span 671 days. The largest gaps in the Year 2 temporal coverage are 18 days (JD 2,448,102–JD 2,448,120), which was unfortunately during a period of moderate activity, and 16 days (JD 2,447,868–JD 2,447,884). The general characteristics of the Year 1, Year 2, and combined data bases are summarized in Table 9. The fractional variation F_{var} is, as defined in Paper I, the ratio of the rms fluctuation to the mean flux, and is corrected for the effect of measurement errors. The parameter R_{max} is the ratio of maximum to minimum flux. Neither of these parameters has been adjusted for the effects of nonvarying components, such as the stellar continuum or the Hβ narrow line.

4.2. *Time-Series Analysis*

Figures 2 and 3 clearly demonstrate that the Hβ emission line shows the same qualitative pattern of variability as the continuum, but with a small time delay. We can quantify this time delay, or lag, by performing a cross-correlation of the continuum and emission-line light curves. This can be carried out in a number of ways, and in Figure 4 we show the cross-correlation function computed by two independent methods, the interpolation method of Gaskell & Sparke (1986; see also Gaskell & Peterson 1987), and the discrete correlation function (DCF) method of Edelson & Krolik (1988). For these data, the

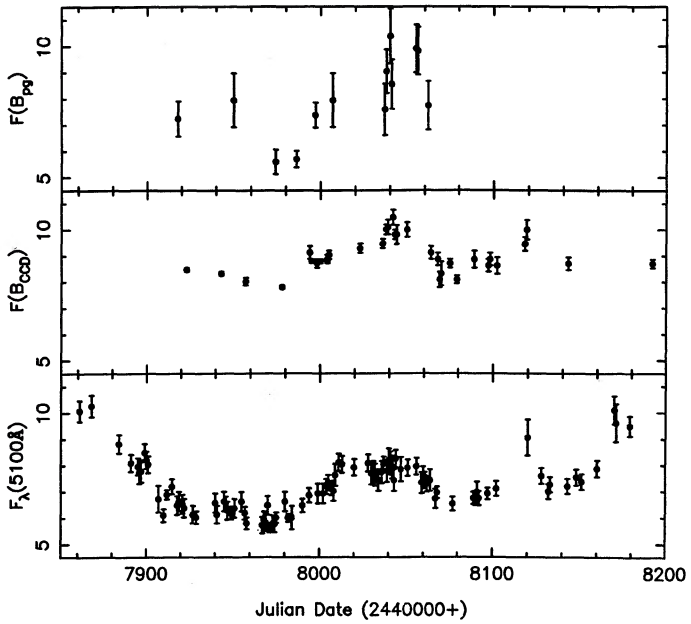

FIG. 1.—The top two panels show the photometric B magnitudes from Tables 2 and 3, respectively, placed on an approximate linear flux scale by using eq. (3). The bottom panel shows the continuum fluxes at 5100 Å (rest frame) from the optical spectra, as given in Table 8. Fluxes are in units of 10^{-15} ergs s^{-1} cm^{-2} $Å^{-1}$.

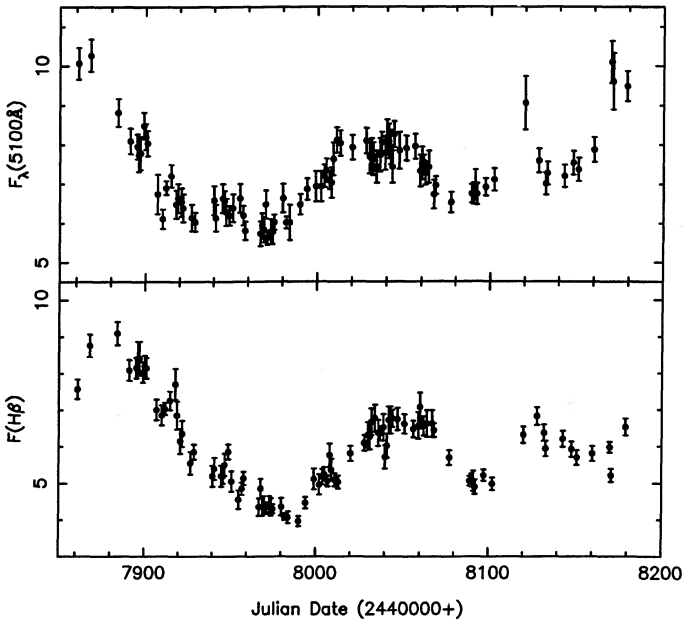

FIG. 2.—Optical continuum (5100 Å) and Hβ emission-line light curves are shown for the Year 2 data. The continuum fluxes are in units of 10^{-15} ergs s^{-1} cm^{-2} $Å^{-1}$ and the emission-line fluxes are in units of 10^{-13} ergs s^{-1} cm^{-2}.

two methods give results which are in close agreement. The lag, as given by the interpolation method, is given in Table 10 for the Year 1 and Year 2 data. The parameter r_{max} is the peak value of the cross-correlation function, which occurs at a time delay Δt_{peak}, and Δt_{cent} refers to the centroid of this function (Koratkar & Gaskell 1991). The uncertainties in these values are typically ~2–3 days. We caution against ascribing much physical significance to this single number, however, as interpretation of both the lag and its uncertainty depends on numerous factors, including the geometry of the BLR and on the continuum behavior (cf. Robinson & Pérez 1990). The relatively small uncertainty in the lag shows that it is, however, a well-defined and experimentally repeatable quantity. In order to extract more information about the geometry of the BLR other than the scale length given by the lag, methods beyond the scope of this work must be employed to solve for the emission-line transfer function (Blandford & McKee 1982), as has been done in the case of the Year 1 data by Krolik et al. (1991) and Horne, Welsh, & Peterson (1991).

In Figure 5, we show the interpolated cross-correlation function and the corresponding continuum autocorrelation function. The continuum autocorrelation function for the Year 2 data is significantly broader than for the Year 1 data (Fig. 8 of Paper II) because the continuum variations were relatively slower during the second year.

We note that some of the continuum and emission-line fluxes in Table 9 are considerably less certain than others because some of the individual data bases are very small. In particular, there are several individual sources which contain only a single spectrum. For the sake of caution, we thus investigate the effect of restricting our time-series analysis to the larger, more reliably intercalibrated data sets (specifically, sets A, F, H, and N, all of which are reasonably large and have considerable overlap with one another). This reduces the total number of epochs from 94 to 86. The cross-correlation result for this subset is also given in Table 10.

5. CONCLUSIONS

In this contribution, we have presented an extension of the NGC 5548 spectroscopic monitoring program described in

TABLE 9

VARIABILITY PARAMETERS AND SAMPLING CHARACTERISTICS

FEATURE (1)	NUMBER OF EPOCHS (2)	SAMPLING INTERVAL (days) Average (3)	SAMPLING INTERVAL (days) Median (4)	MEAN FLUX[a] (5)	F_{var} (6)	R_{max} (7)
F_λ(5100 Å), Year 1	126	3.4	1	9.95	0.126	2.36
F_λ(5100 Å), Year 2	94	4.4	2	7.25	0.133	1.83
F_λ(5100 Å), combined	220	4.1	2	8.80	0.199	2.42
Hβ, Year 1	132	3.3	1	8.62	0.095	1.57
Hβ, Year 2	94	4.4	2	5.98	0.191	2.30
Hβ, combined	226	4.0	1	7.52	0.215	2.67

[a] Units as in Table 8.

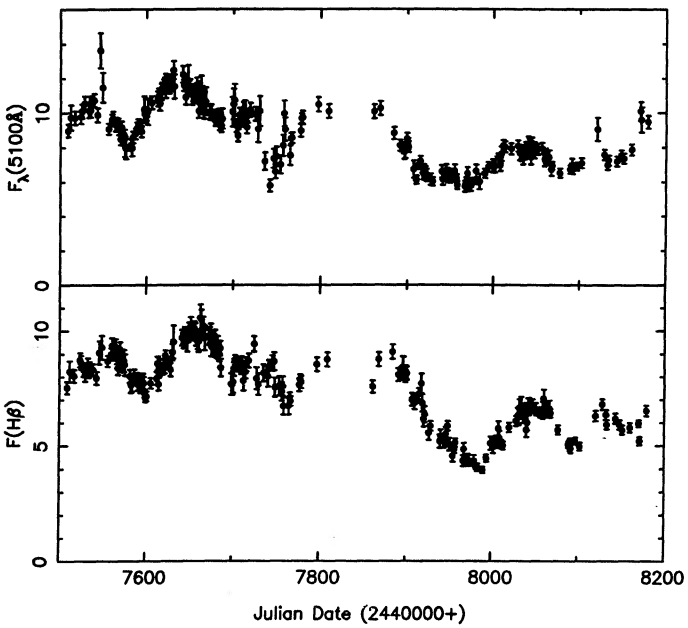

FIG. 3.—Optical continuum (5100 Å) and Hβ emission-line light curves are shown for both years of the NGC 5548 monitoring campaign. The Year 2 data are from Table 8 and the Year 1 data are from Table 12. The continuum fluxes are in units of 10^{-15} ergs s^{-1} cm^{-2} $Å^{-1}$ and the emission-line fluxes are in units of 10^{-13} ergs s^{-1} cm^{-2}.

Papers I and II. We have verified the principal result of Paper II, namely that the Hβ emission line responds to optical continuum variations on a time scale of order ~20 days. The cross-correlation results for Year 1 (Δt_{peak} = 17 days, Δt_{cent} = 19.4 days) and Year 2 (Δt_{peak} = 18 days, Δt_{cent} = 18.8 days) are remarkably consistent with one another. The continuum was generally fainter, by 25% on average, during Year 2 than during Year 1, and the galaxy passed through an extremely faint state during 1990 February–April.

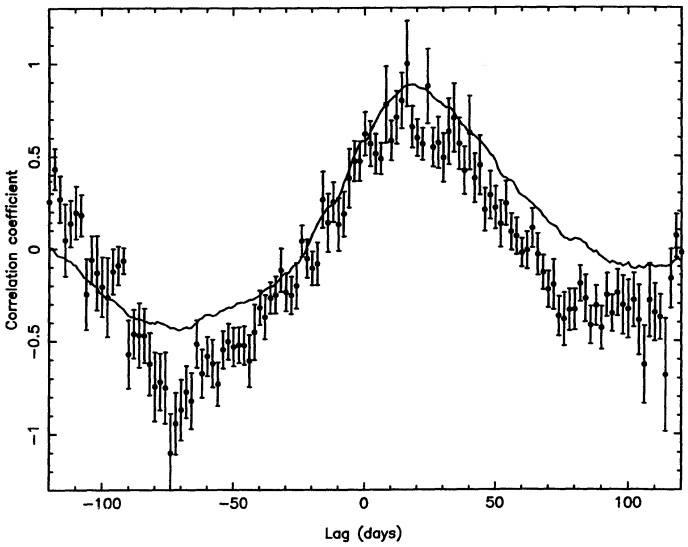

FIG. 4.—The interpolation cross-correlation function, shown as a smooth line, and the discrete correlation function (DCF), shown as individual points with associated uncertainties, for the optical continuum (5100 Å) and the Hβ emission line, computed from the data given in Table 8. The bin width for the DCF is 2 days, since the intercalibration process smooths out variations on shorter time scales. The Hβ emission line lags the optical continuum by ~19 days. The cross-correlation function is broad and flat topped; this is attributable to the width of the continuum autocorrelation function, shown in Fig. 5.

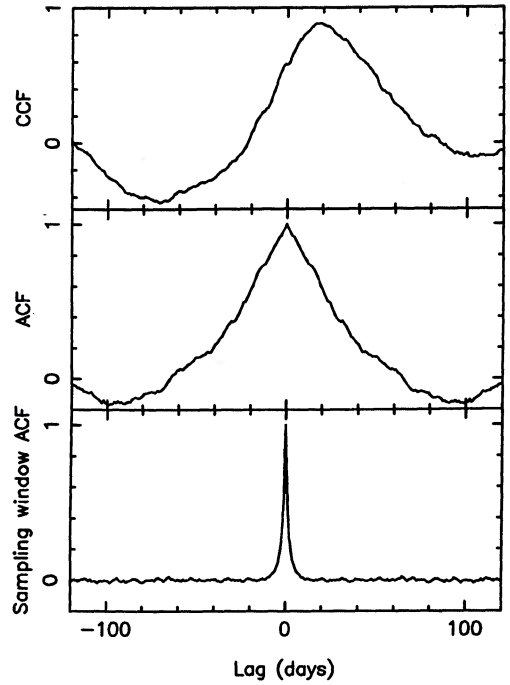

FIG. 5.—The top panel shows the optical continuum–Hβ cross-correlation function. The optical continuum autocorrelation function is given for comparison in the middle panel. The sampling window autocorrelation function, which shows the effect of interpolating the data between observations (Gaskell & Peterson 1987), is shown in the bottom panel.

Additional observations from Year 1 (Appendix B), and the optical continuum light curve at 5100 Å for Year 1 (Appendix A) also have been presented.

The present work and Paper II constitute a first look at the NGC 5548 optical monitoring data, and as such have concentrated solely on the important questions of the behavior of the optical continuum and the Hβ emission line. However, this program is providing an extended high-quality data base for planned studies of the long-term behavior of the optical continuum, flux variations in other optical emission lines, and emission-line profile variations. The results of these studies will be reported in future contributions.

We are very grateful to the Directors and Telescope Allocation Committees of our various observatories for their support of this project. Individual investigators have benefited from support from a number of agencies, including the following: the National Science Foundation: AST-8915258 (Ohio State University), AST-8821839 (University of Florida), AST-8714937 (University of Texas), AST-8957063 and AST-9003829 (University of California, Berkeley), AST-8614510 (University of California), and USE-8750955 (Colgate University, under the College Science Instrumentation Program); NASA: NAG5-1366 (Ohio State Univ.), NAS8-30751 (Center for Astrophysics); BMFT grant Verbundforschung Astronomie FKZ 05 5GO42A1 (Universitäts-Sternwarte Göttingen); the American Astronomical Society Small Grants Program (Colgate University); the Centre National de la Recherche Scientifique and the Ministere de la Recherche et Technologie. The Isaac Newton and William Herschel telescopes are run by the Royal Greenwich Observatory at the Spanish Observatorio del Roque de los Muchachos of the Instituto de Astrofísica de Canarias. J. P. Halpern is thanked for the contribution of an Hα spectrum (n57945o) to the data base.

TABLE 10

CROSS-CORRELATION RESULTS
OPTICAL CONTINUUM vs. Hβ

Data Set (1)	Δt_{peak} (days) (2)	Δt_{cent} (days) (3)	r_{max}
Year 1, Paper II	19	18.2	0.85
Year 1, revised continuum	19	19.1	0.84
Year 1, revised continuum + new data	17	19.4	0.84
Year 2 (Table 8)	18	18.8	0.88
Year 2, best-calibrated data	16	18.0	0.92

APPENDIX A

5100 Å CONTINUUM MEASUREMENTS FOR YEAR 1

In Paper II, the optical continuum values reported are those measured at a rest wavelength of 4870 Å, i.e., directly underneath the Hβ emission line. The continuum flux at this wavelength was determined by interpolating underneath the Hβ emission with a straight line. The primary factor in the decision to use this particular continuum point is that it appears in all of the spectra which also contain the Hβ line; in particular, a few of the Hβ-region spectra reported in Paper II cut off shortward of 5100 Å.

In order to facilitate a better comparison of the behavior of the optical continuum with that of the ultraviolet continuum and to evaluate the contribution of the underlying starlight to the optical spectra, it is desirable to use a continuum point which is more free of line emission than the 4870 Å point. A particular worry about the 4870 Å measurements is that the short-wavelength window used in the continuum definition (i.e., at ~4780 Å) may be significantly contaminated by He II λ4686 emission. We have therefore remeasured the optical continuum from the spectra reported in Paper II. We have remeasured the continuum in a narrow window (i.e., ~10–15 Å wide) at the local minimum in the spectrum between the Hβ + [O III] complex and the Fe II λ5250 blend, i.e., at ~5100 Å. Remeasurement of all of the spectra necessitated re-evaluation of the extended source intercalibration constant G (eq. [2]). The point-source intercalibration constant φ is determined from the emission-line ratios, and is not a function of the continuum measurement, so the values from Paper II still apply. The revised values of G, which are appropriate for the 5100 Å continuum, are given in Table 11.

The revised optical continuum and Hβ light curves are given in Table 12; the light curves presented here supersede those given in Table 9 of Paper II. It should be noted that the additional Year 1 data reported in Appendix B have been included in Table 12. It should also be noted that there are a few blank continuum entries in column (2) of Table 12; these represent data from which the Hβ emission-line flux could be measured, but the spectrum cuts off shortward of 5100 Å.

The 4870 Å and 5100 Å continuum measurements for the Year 1 data are compared directly in Figure 6. A least-squares fit to these data gives the relationship

$$F_{4870} = (1.236 \pm 0.027)F_{5100} - (0.995 \pm 0.274) \times 10^{-15} . \quad (4)$$

TABLE 11

EXTENDED SOURCE CORRECTION FOR
YEAR 1 5100 Å CONTINUUM

Data Set (1)	G (10^{-15} ergs s^{-1} cm^{-2} Å^{-1}) (2)
A	0.000
B	5.642 ± 0.709
C	0.225 ± 0.693
E	−0.154 ± 0.490
F	−1.831 ± 0.363
G	0.000
H1	0.341 ± 0.820
H2	−1.128 ± 0.861
I	0.388 ± 0.898
J	2.269 ± 0.351
K1	−0.347 ± 0.132
K2	−1.106 ± 1.237
M	−0.682 ± 0.693
N1	1.392 ± 0.947
N2	1.023 ± 0.720
O	−1.424 ± 0.303
P	2.701 ± 0.349
Q	−1.472 ± 0.533

TABLE 12

YEAR 1 REVISED OPTICAL CONTINUUM AND Hβ LIGHT CURVES

Julian Date (2,440,000+) (1)	F_λ(5100 Å) (10^{-15} ergs s^{-1} cm^{-2} Å^{-1}) (2)	F(Hβ) (10^{-13} ergs s^{-1} cm^{-2}) (3)	Julian Date (2,440,000+) (1)	F_λ(5100 Å) (10^{-15} ergs s^{-1} cm^{-2} Å^{-1}) (2)	F(Hβ) (10^{-13} ergs s^{-1} cm^{-2}) (3)
7509.....	8.98 ± 0.36	7.53 ± 0.26	7649.....	11.48 ± 0.38	9.82 ± 0.31
7512.....	9.73 ± 0.73	8.24 ± 0.45	7650.....	11.49 ± 0.46	10.11 ± 0.25
7517.....	9.71 ± 0.39	8.03 ± 0.28	7652.....	11.07 ± 0.83	10.27 ± 0.41
7524.....	9.79 ± 0.39	8.74 ± 0.31	7653.....	11.10 ± 0.44	10.04 ± 0.35
7525.....	10.11 ± 0.40	8.63 ± 0.30	7654.....	11.09 ± 0.31	9.81 ± 0.20
7528.....	10.56 ± 0.42	8.31 ± 0.29	7655.....	11.16 ± 0.37	10.07 ± 0.28
7530.....	...	8.09 ± 0.28	7656.....	11.15 ± 0.39	10.12 ± 0.30
7533.....	10.14 ± 0.41	8.52 ± 0.30	7657.....	11.05 ± 0.44	9.99 ± 0.35
7534.....	10.55 ± 0.42	8.26 ± 0.29	7658.....	11.63 ± 0.40	9.63 ± 0.27
7535.....	10.16 ± 0.41	8.37 ± 0.29	7660.....	10.11 ± 0.40	9.54 ± 0.33
7539.....	10.74 ± 0.38	8.31 ± 0.25	7661.....	11.35 ± 0.45	9.56 ± 0.48
7543.....	9.88 ± 0.40	7.95 ± 0.28	7663.....	11.30 ± 0.85	10.56 ± 0.58
7546.....	13.62 ± 1.02	9.05 ± 0.50	7664.....	10.72 ± 0.80	10.50 ± 0.42
7549.....	11.48 ± 0.86	9.28 ± 0.51	7665.....	10.75 ± 0.45	9.92 ± 0.26
7556.....	9.08 ± 0.32	8.69 ± 0.24	7666.....	10.43 ± 0.78	10.21 ± 0.41
7560.....	9.59 ± 0.34	8.99 ± 0.26	7668.....	10.66 ± 0.80	9.69 ± 0.53
7561.....	9.69 ± 0.39	9.37 ± 0.33	7673.....	9.99 ± 0.40	9.72 ± 0.34
7564.....	9.31 ± 0.37	9.04 ± 0.32	7674.....	10.09 ± 0.40	9.82 ± 0.34
7565.....	9.36 ± 0.37	9.32 ± 0.33	7675.....	...	9.86 ± 0.44
7567.....	9.31 ± 0.37	8.88 ± 0.31	7676.....	...	9.31 ± 0.42
7568.....	9.09 ± 0.36	8.38 ± 0.29	7678.....	9.79 ± 0.28	9.35 ± 0.21
7570.....	8.48 ± 0.34	9.19 ± 0.32	7679.....	9.62 ± 0.38	9.28 ± 0.27
7571.....	9.16 ± 0.37	8.52 ± 0.30	7680.....	9.78 ± 0.39	9.76 ± 0.29
7572.....	8.48 ± 0.34	8.77 ± 0.31	7681.....	9.62 ± 0.38	9.28 ± 0.23
7573.....	8.54 ± 0.23	8.98 ± 0.23	7682.....	9.68 ± 0.39	9.04 ± 0.22
7574.....	8.74 ± 0.31	8.44 ± 0.25	7683.....	9.83 ± 0.39	9.45 ± 0.33
7575.....	8.05 ± 0.60	8.70 ± 0.48	7684.....	9.36 ± 0.38	9.09 ± 0.32
7576.....	7.94 ± 0.60	8.53 ± 0.47	7685.....	9.52 ± 0.38	8.99 ± 0.31
7582.....	8.15 ± 0.33	8.03 ± 0.28	7686.....	9.26 ± 0.37	9.25 ± 0.32
7583.....	7.98 ± 0.48	7.66 ± 0.34	7687.....	9.65 ± 0.58	8.40 ± 0.38
7584.....	8.59 ± 0.34	7.76 ± 0.39	7699.....	10.05 ± 0.86	7.68 ± 0.46
7587.....	8.79 ± 0.31	8.09 ± 0.24	7700.....	10.50 ± 0.89	7.68 ± 0.46
7589.....	9.12 ± 0.32	7.91 ± 0.23	7701.....	10.75 ± 0.91	7.78 ± 0.47
7590.....	9.26 ± 0.37	7.95 ± 0.23	7702.....	...	8.34 ± 0.29
7591.....	9.26 ± 0.37	7.69 ± 0.27	7703.....	9.26 ± 0.37	8.73 ± 0.22
7592.....	9.31 ± 0.25	7.83 ± 0.18	7705.....	8.69 ± 0.35	8.57 ± 0.30
7593.....	9.16 ± 0.26	7.91 ± 0.20	7707.....	9.88 ± 0.40	8.52 ± 0.30
7594.....	8.92 ± 0.31	7.53 ± 0.22	7708.....	9.57 ± 0.38	8.57 ± 0.30
7597.....	10.20 ± 0.76	7.72 ± 0.42	7709.....	9.57 ± 0.38	8.52 ± 0.30
7598.....	9.94 ± 0.40	7.74 ± 0.27	7710.....	9.73 ± 0.34	8.35 ± 0.23
7599.....	9.88 ± 0.40	7.28 ± 0.18	7711.....	10.21 ± 0.41	8.64 ± 0.25
7600.....	9.84 ± 0.28	7.09 ± 0.17	7713.....	9.97 ± 0.75	7.83 ± 0.43
7601.....	10.08 ± 0.76	7.16 ± 0.21	7715.....	9.16 ± 0.37	8.21 ± 0.29
7606.....	10.60 ± 0.37	7.73 ± 0.23	7716.....	9.81 ± 0.39	8.54 ± 0.30
7613.....	10.80 ± 0.43	7.94 ± 0.28	7719.....	10.16 ± 0.41	8.70 ± 0.31
7614.....	10.99 ± 0.44	8.59 ± 0.30	7725.....	9.93 ± 0.40	9.43 ± 0.33
7615.....	10.56 ± 0.42	7.69 ± 0.27	7728.....	9.06 ± 0.77	7.93 ± 0.48
7616.....	...	8.41 ± 0.38	7730.....	10.10 ± 0.86	7.68 ± 0.46
7617.....	11.23 ± 0.45	8.47 ± 0.30	7736.....	7.18 ± 0.50	8.18 ± 0.37
7618.....	11.43 ± 0.32	8.30 ± 0.20	7741.....	...	8.01 ± 0.44
7620.....	11.55 ± 0.38	8.33 ± 0.23	7742.....	5.78 ± 0.35	8.35 ± 0.38
7621.....	11.66 ± 0.41	8.36 ± 0.23	7746.....	7.36 ± 0.55	8.59 ± 0.34
7622.....	11.56 ± 0.69	8.54 ± 0.38	7748.....	6.60 ± 0.40	8.68 ± 0.39
7623.....	11.70 ± 0.47	8.93 ± 0.22	7749.....	7.47 ± 0.56	7.54 ± 0.41
7624.....	11.70 ± 0.47	8.68 ± 0.22	7754.....	7.01 ± 0.53	7.60 ± 0.42
7626.....	11.60 ± 0.46	8.67 ± 0.22	7757.....	8.11 ± 0.61	7.37 ± 0.41
7627.....	11.87 ± 0.34	8.67 ± 0.22	7758.....	9.97 ± 0.75	7.60 ± 0.42
7628.....	11.83 ± 0.41	8.63 ± 0.24	7759.....	9.04 ± 0.68	6.73 ± 0.37
7629.....	11.73 ± 0.47	8.32 ± 0.29	7765.....	7.53 ± 0.56	6.73 ± 0.37
7631.....	12.48 ± 0.53	9.09 ± 0.35	7766.....	8.51 ± 0.31	7.10 ± 0.22
7632.....	11.53 ± 0.69	9.53 ± 0.71	7767.....	8.55 ± 0.30	6.94 ± 0.20
7642.....	12.22 ± 0.49	9.71 ± 0.34	7777.....	8.98 ± 0.36	7.64 ± 0.27
7643.....	11.58 ± 0.33	9.66 ± 0.24	7778.....	9.70 ± 0.27	7.91 ± 0.20
7644.....	11.77 ± 0.31	9.49 ± 0.24	7779.....	9.74 ± 0.39	7.78 ± 0.27
7645.....	10.91 ± 0.44	9.81 ± 0.34	7797.....	10.48 ± 0.42	8.54 ± 0.30
7648.....	11.88 ± 0.89	9.63 ± 0.53	7809.....	10.09 ± 0.40	8.76 ± 0.31

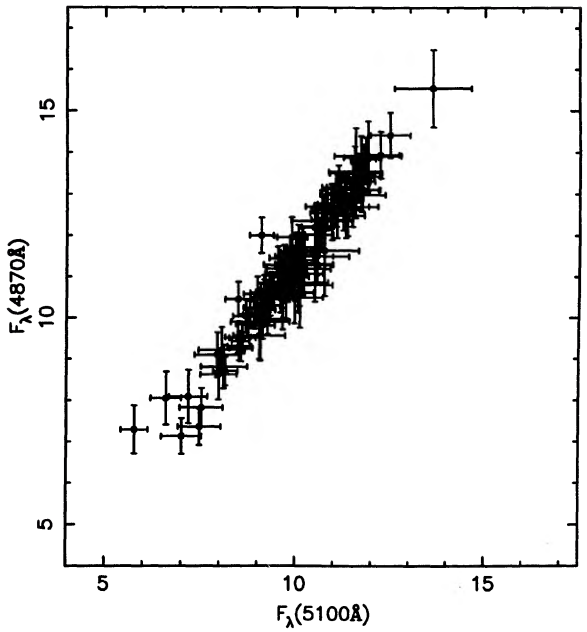

FIG. 6.—Comparison of the continuum measurements at 5100 Å (from Table 12) and at 4870 Å (from Table 9 of Paper II) for the Year 1 spectra. Fluxes are in units of 10^{-15} ergs s^{-1} cm^{-2} $Å^{-1}$.

The optical continuum–Hβ cross-correlation result for the light curves given in Table 12 is given in Table 10. We note that the centroid of the cross-correlation function is rather insensitive to the details of the light curve, but the location of the *peak* of the cross-correlation function Δt_{peak} can easily be displaced by a few days with small changes in the light curve. This is a consequence of the cross-correlation function being so flat-topped (see Fig. 4). The difference between the value $\Delta t_{peak} = 17$ given in Table 10 and the corresponding value given in Paper II ($\Delta t_{peak} = 19$) is an illustration of this; this difference arises *not* from the continuum redefinition, but from the inclusion of the five new data points from Appendix B.

APPENDIX B

ADDITIONAL DATA FROM YEAR 1

Several spectra obtained during Year 1 were not reduced in time for inclusion in Paper II, and we therefore report on these data here. A log of these additional observations is given in Table 13, which follows the same format as Table 1.

TABLE 13

ADDITIONAL SPECTROSCOPIC OBSERVATIONS FROM YEAR 1

UT Date (1)	Julian Date (2,440,000+) (2)	Code (3)	Aperture Size (4)	Aperture P.A. (5)	Seeing (6)	Resolution (Å) (7)	Range (Å) (8)	IRAF File (9)
1989 May 1	7647	J	1.5 × 7.6	90	1″.5	10	6060–8790	n57647j
1989 May 1	7648	M	2.1 × 10.0	0	3	2	6450–6790	n57648mb
1989 May 2	7648	J	4.0 × 7.6	90	1.5	10	6060–8790	n57648j
1989 May 5	7652	M	2.1 × 10.0	0	1	2	4740–5300	n57652ma
1989 May 5	7652	M	2.1 × 10.0	0	1	2	6450–6790	n57652mb
1989 May 9	7656	M	2.4 × 10.0	0	2	2	6450–6790	n57656mb
1989 May 17	7664	M	2.1 × 10.0	0	2–3	5	3680–5890	n57664ma
1989 May 17	7664	M	2.1 × 10.0	0	2–3	8	5620–7150	n57664mb
1989 May 18	7665	M	2.1 × 10.0	0	2	2	4750–5310	n57665ma
1989 May 18	7665	M	2.1 × 10.0	0	2	3	6490–6990	n57665mb
1989 May 19	7666	M	2.1 × 10.0	0	1.5–2	2	4750–5310	n57666ma
1989 May 19	7666	M	2.1 × 10.0	0	1.5–2	3	6490–6990	n57666mb
1989 Jun 13	7691	M	2.1 × 10.0	0	2–3	4	3880–4910	n57691ma
1989 Jun 13	7691	M	2.1 × 10.0	0	2–3	4	6300–7300	n57691mb
1989 Jun 20	7697	M	2.4 × 10.0	0	1.5	2	6530–6770	n57697m
1989 Jun 22	7700	M	1.2 × 10.0	0	1	2	6530–6770	n57700m
1989 Jul 5	7713	M	1.2 × 10.0	0	3	4	6240–6930	n57713mb
1989 Aug 7	7746	M	1.5 × 10.0	0	1.5	11	3840–7180	n57746m
1989 Aug 15	7754	M	2.1 × 10.0	0	1.5	3	6490–6990	n57754mb
1989 Aug 30	7769	M	2.4 × 10.0	0	3	11	5560–8920	n57769m

TABLE 14

MEASUREMENTS OF ADDITIONAL YEAR 1 SPECTRA

Julian Date (2,440,000+) (1)	$100F_\lambda$(5100 Å) / F([O III] λ5007) (2)	F(Hβ) / F([O III] λ5007) (3)	IRAF File (4)
	M—Calar Alto CCD		
7652.....	1.79	1.77	n57652ma
7664.....	1.73	1.81	n57664ma
7665.....	1.67	1.83	n57665ma
7666.....	1.68	1.76	n57666ma
7746.....	1.15	1.48	n57746m

TABLE 15

SCALED FLUX MEASUREMENTS FROM ADDITIONAL YEAR 1 SPECTRA

Julian Date (2,4000,000+) (1)	F_λ(5100 Å) (10^{-15} ergs ergs s^{-1} cm^{-2} $Å^{-1}$) (2)	F(Hβ) (10^{-13} ergs s^{-1} cm^{-2}) (3)
7652.....	11.07 ± 0.83	10.27 ± 0.41
7664.....	10.72 ± 0.80	10.50 ± 0.42
7665.....	10.37 ± 0.78	10.62 ± 0.22
7666.....	10.43 ± 0.78	10.21 ± 0.41
7746.....	7.36 ± 0.55	8.59 ± 0.34

Five of the spectra, all from set M, cover the Hβ spectral region. The flux ratios F_λ(5100 Å)/F([O III] λ5007) and F(Hβ)/F([O III] λ5007) are given in Table 14 for these spectra. The 5100 Å continuum and Hβ fluxes have been placed on an absolute scale by using equations (1) and (2) with the point-source calibration constant φ for set M taken from Table 7 of Paper II and the extended source constant G from Table 6 of this paper; these values are presented in Table 15, and have been included in the revised Year 1 light curve given in Table 12.

REFERENCES

Beckert, D. C., & Newberry, M. V. 1989, PASP, 101, 849
Blandford, R. D., & McKee, C. F. 1982, ApJ, 255, 419
Clavel, J., et al. 1991, ApJ, 366, 64 (Paper I)
Edelson, R. A., & Krolik, J. H. 1988, ApJ, 333, 646
Gaskell, C. M., & Peterson, B. M. 1987, ApJS, 65, 1
Gaskell, C. M., & Sparke, L. S. 1986, ApJ, 305, 175
Horne, K., Welsh, W. F., & Peterson, B. M. 1991, ApJ, 367, L5
Koratkar, A. P., & Gaskell, C. M. 1991, ApJS, 75, 719
Krolik, J. H., Horne, K., Kallman, T. R., Malkan, M. A., Edelson, R. A., & Kriss, G. A. 1991, ApJ, 371, 541
Oke, J. B., & Gunn, J. E. 1983, ApJ, 266, 713
Penston, M. J., Penston, M. V., & Sandage, A. 1971, PASP, 83, 783
Peterson, B. M., et al. 1991, ApJ, 368, 119 (Paper II)
Robinson, A., & Pérez, E. 1990, MNRAS, 244, 138